Ab initio study of surface self-segregation effect on the adsorption of oxygen on the γ-TiAl(111) surface

Shi-Yu Liu,[1] Jia-Xiang Shang,[1,*] Fu-He Wang,[2] and Yue Zhang[1]
[1]*School of Materials Science and Engineering, Beijing University of Aeronautics and Astronautics, Beijing 100083, People's Republic of China*
[2]*Department of Physics, Capital Normal University, Beijing 100037, People's Republic of China*
(Received 5 October 2008; revised manuscript received 13 January 2009; published 10 February 2009)

The effects of surface self-segregation on the adsorption of oxygen on the γ-TiAl(111) surface are investigated by density-functional theory calculations. The oxygen binding-energy results show that on the pure γ-TiAl(111) surface, the most stable adsorption sites of oxygen atoms are the sites with more Ti sites as their neighbors, which is in agreement with previous calculations. The defect formation energies and the relative surface energies as functions of chemical potential of Al are calculated. Furthermore, the phase diagram of γ-TiAl(111) surfaces with different defects and different oxygen coverage is also calculated. The calculated results show that Al atom can segregate at the γ-TiAl(111) surface. Especially, at high Al chemical potential, the first surface layer of the γ-TiAl(111) surface can be composed of Al atoms. In this case, the oxygen adsorption behavior is very similar to the case of Al(111) surface: the binding energy per oxygen atom decreases with the increase in the oxygen coverage due to an attractive interaction between O atoms. These results show that the occurrence of Al self-segregation at the γ-TiAl(111) surface can enhance the interaction between O and Al atoms. The Al surface segregation effect may be the reason why the growth of pure alumina layer resulting from the selective oxidation of aluminum formed on γ-TiAl(111) surface at the first stage in the experiments.

DOI: 10.1103/PhysRevB.79.075419 PACS number(s): 68.43.Bc, 71.15.Mb, 81.65.Mq

I. INTRODUCTION

γ-TiAl-based intermetallic compounds are attracting more and more attention recently due to their merits of low density, high specific strength, and relatively good properties at elevated temperatures. Therefore they are being considered as prospective structural materials for applications in aerospace and automobile industries.[1–3] However, their practical applications are still hindered by low oxidation resistance at high temperatures. This is due to the growth of mixed oxide layer formed by competitive oxidation of the Ti and Al alloying elements,[4–8] which prevents the formation of a continuous and dense α alumina that would provide a more effective oxidation barrier in high-temperature applications. Whether a dense protective layer of Al_2O_3 is formed or a fast growing scale depends on the local activities of the metals and the oxides, which are influenced mainly by the oxygen partial pressure, temperature, and also by alloying elements.[9,10]

Recently, Maurice *et al.*[11–13] studied the initial stages of oxidation of the γ-TiAl(111) surface at 650 °C under low oxygen pressure by x-ray photoelectron spectroscopy (XPS), scanning tunneling microscopy (STM), and Auger-electron spectroscopy (AES). They found that an ultrathin γ-like Al_2O_3(111) film on the γ-TiAl(111) surface was produced by oxidizing at the first stage.[11] Then they also found the first regime of oxidation characterized by the growth of a pure alumina layer resulting from the selective oxidation of aluminum, followed by a second regime of simultaneous oxidation of both metal elements.[12] On the theory side, Li *et al.*[14] performed first-principles total-energy calculations for the oxygen adsorption on the pure γ-TiAl(111) surface. They found the most favorable site for oxygen is the adsorption site with more Ti atoms as its nearest neighbors on the surface layer at all coverage.[14] However, their result could not give an explanation of the above experiment.[11–13]

Surface segregation is very important for alloys and intermetallics. Recently, it was shown by Blum *et al.*[15] that even a slight deviation from the ideal stoichiometry in the bulk can drastically affect the composition of the binary CoAl(100) surface as a result of the strong tendency for Co antisites to surface segregation. Pourovskii *et al.*[16] also demonstrated that a small deviation from stoichiometry in bulk composition can strongly affect the composition of the (111) surface of an NiPt alloy below its order-disorder transition temperature. Lozovoi *et al.*[17] performed *ab initio* study of the initial oxidation of NiAl(110) surface. They found that the thin oxide film is hugely stabilized by the segregation of Al antisites and Ni vacancies, and they developed scenarios involving segregation of point defects to the surface as a result of the oxidation.[17]

These interesting segregation behaviors motivate us to investigate the surface segregation effect on the adsorption of oxygen on the γ-TiAl(111) surface, which is also a step to understand the formation of surface oxide. At first, we will investigate the surface self-segregation of the clean γ-TiAl(111) surface. Then, we will study the effects of surface segregation on oxygen adsorption on the γ-TiAl(111) surface in order to understand the above-mentioned experimental results.[11–13] The remainder of this paper is organized as follows. The calculational method and models, as well as the thermodynamical method, are introduced in Sec. II. In Sec. III, the surface self-segregation behavior at the clean γ-TiAl(111) surface is analyzed. Section IV gives the results for oxygen adsorbed on the pure γ-TiAl(111) surface and segregated γ-TiAl(111) with Al antisites. Finally, our results are summarized in Sec. V.

 ©2009 The American Physical Society

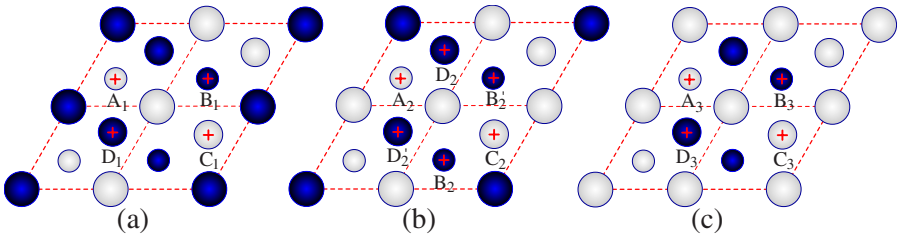

FIG. 1. (Color online) Top view of the γ-TiAl(111)-(2×2) surface with possible oxygen adsorption sites for three cases: (a) pure γ-TiAl(111)-(2×2) surface, (b) γ-TiAl(111)-(2×2) surface with one Al antisite defect [denoted by γ-TiAl(111)-(2×2)-1Al], (c) γ-TiAl(111)-(2×2) surface with two Al antisites defect [denoted by γ-TiAl(111)-(2×2)-2Al]. Large, medium, and small blue and gray balls represent the Ti and Al atoms in the first, second, and third surface layers, respectively. The cross "+" represents oxygen atom. The symbols *A*, *B*, *C*, and *D* denote fcc-Al, fcc-Ti, hcp-Al, and hcp-Ti sites, respectively. The subscript numbers 1, 2, and 3 represent these three cases, and the prime " ′" in (b) denotes the same sites as that on the pure surface, but the surrounding atom in the first surface layer is changed from Ti to Al.

II. COMPUTATIONAL METHOD AND MODELS

The calculations presented in this paper are based on the density-functional theory (DFT) (Refs. 18 and 19) and performed by means of the plane-wave-pseudopotential Vienna *ab initio* simulation package (VASP) (Refs. 20–22) codes. For the exchange-correction energy functional, the generalized gradient approximation (GGA) (Ref. 23) is employed. The projector augmented wave method proposed by Blöchl[24] and implemented by Kresse and Joubert[25] is used. We tested kinetic-energy cutoff and *k*-point sampling convergence for all supercells. As a result of the convergence tests, we use a kinetic-energy cutoff of 400 eV for all calculations. For bulk γ-TiAl, which has a face-centered tetragonal (fct) $L1_0$ crystal structure with alternate (001) planes of Ti and Al atoms, a 15×15×15 *k*-point mesh for the primitive cell is used. The calculated lattice constants are a=3.980 Å and c=4.086 Å, which agree well with experiment[26] and previous DFT-GGA results.[27]

All the γ-TiAl(111) surfaces were modeled by a slab of seven metal slab layers separated by a vacuum region equivalent to seven bulk metal layers. The surface calculations were done in 2×2 surface unit cells with 9×9×1 Monkhorst-Pack *k* points in the Brillouin zone. Oxygen is placed on one side of the slab where the induced dipole moment is taken into account by applying a dipole correction.[28,29] There are four atoms (two Ti atoms and two Al atoms) each layer in the surface cell. Here, the coverage of oxygen Θ is defined as the ratio of the number of adsorbed oxygen atoms to the number of atoms in an ideal substrate layer. In the calculation, the bottom three metal layers were fixed at their bulk truncated structure. The other atoms were relaxed until the forces on each of them were less than 0.01 eV/Å. At the first step, we calculate the nine different adsorption sites for oxygen on the clean γ-TiAl(111)-(2×2) surface at the oxygen coverage of 0.25 monolayer (ML). The top site is on top of a Ti atom or Al atom and the bridge site is in the middle of two substrate atoms in the top layer hexagonal-close-packed (hcp) sites where the oxygen is in threefold hollow sites with a Ti atom (hcp-Ti site) or Al atom (hcp-Al site) in the second layer under the oxygen atom and face-centered cubic (fcc) sites where the oxygen is in threefold hollow sites with a Ti atom (fcc-Ti site) or Al atom (fcc-Al site) in the third layer under the oxygen atom. The four sites fcc-Al, fcc-Ti, hcp-Al, and hcp-Ti are more stable than the other sites. In the following, we just discuss the four sites as well as their combination. The four oxygen adsorption sites are shown in Fig. 1, where the adsorption sites fcc-Al, fcc-Ti, hcp-Al, and hcp-Ti are denoted by A, B, C, and D, respectively. Figures 1(a)–1(c) represent the adsorption sites on the γ-TiAl(111)-(2×2) surface with none antisite defect (pure surface), one Al antisite defect, and two Al antisites defect, respectively. The subscript numbers 1, 2, and 3 represent these three cases and the prime " ′" in Fig. 1(b) denotes the same sites as that on the pure surface, but one of the surrounding atoms in the first surface layer is changed from Ti to Al.

The intermetallic compound γ-TiAl consists of two sublattices: the α sublattice for Ti and the β sublattice for Al. There are four possible kinds of point defects, i.e., vacancy in α, vacancy in β, antisite of Al occupying α, and antisite of Ti occupying β. In order to study the stability of defective system, the defect formation energy E_f of the γ-TiAl(111) surface and γ-TiAl bulk for four kinds of defects is defined as

$$E_f = E_t^d - E_t - \sum_i \Delta N_i E_i, \tag{1}$$

where E_t and E_t^d represent the total energies of the unit cell without and with defect, respectively. ΔN_i represents the increase in the number of atoms of species i of the defective system compared with that of nondefective system. E_i denotes the energy per atom in its bulk state. A 28-atom supercell for the γ-TiAl(111)-(2×2) surface and a 32-atom (2×2×2) supercell for γ-TiAl bulk are used to calculate the defect formation energies at surface and in bulk.

The stability of various the O/γ-TiAl(111) system is analyzed with respect to the average binding energy per oxygen atom. The average binding energy per oxygen atom as a function of the coverage Θ is defined as

$$E_b(\Theta) = \frac{1}{N_O^{\text{atom}}}[E_{O/\text{TiAl}(111)}(\Theta) - (E_{\text{TiAl}(111)} + N_O^{\text{atom}} E_O^{\text{atom}})], \tag{2}$$

where N_O^{atom} is the number of oxygen atoms in the unit cell, $E_{O/\text{TiAl}(111)}$, $E_{\text{TiAl}(111)}$, and E_O^{atom} represent the total energies

TABLE I. The calculated defect formation energy at the γ-TiAl(111) surface with the depth of defective layer and in γ-TiAl bulk (eV).

Layer	E_v(Ti)	E_v(Al)	E_{anti}(Ti)	E_{anti}(Al)	E_{anti}(2Al)
1	1.05	2.08	1.07	−0.64	−0.10
2	1.84	2.85	0.80	0.15	0.50
3	1.81	2.73	0.92	0.20	
Bulk	1.88	2.61	0.83	0.18	

per unit cell of the TiAl(111) slab with oxygen atoms, the clean TiAl(111) slab, and free oxygen atom, respectively. According to the definition of E_b, the interaction between the adsorbed oxygen atoms and surface is enhanced (weakened) when the binding energy decreases (increases). So the lower the binding energy is, the more stable the system is.

The thermodynamic stability of a given surface is determined by its surface energy. The thermodynamics formalism employed follows the scheme of Qian *et al.*,[30] Northrup,[31] Zhang and Wang,[32] and Kitchin *et al.*[33] The surface energy γ can be defined as

$$\gamma = \frac{1}{S_0}[E_{slab} - N_{Ti}\mu_{Ti} - N_{Al}\mu_{Al} - N_O\mu_O - PV - TS]. \quad (3)$$

Here, S_0 is the surface area. E_{slab} is the total energy of the slab and N_{Ti}, N_{Al}, and N_O denote the number of Ti, Al, and O atoms in the slab. The chemical potentials of Ti, Al, and O are represented by μ_{Ti}, μ_{Al}, and μ_O, respectively. We neglect the *TS* term and pressure term contributions for the TiAl surface. Therefore, the surface energy γ can be rewritten as

$$\gamma = \frac{1}{S_0}[E_{slab} - N_{Ti}\mu_{Ti} - N_{Al}\mu_{Al} - N_O\mu_O]. \quad (4)$$

For the pure γ-TiAl(111)-(2×2) surface, we denote the surface energy γ^S as

$$\gamma^S = \frac{1}{S_0}[E^S_{slab} - N^S_{Ti}\mu_{Ti} - N^S_{Al}\mu_{Al}]. \quad (5)$$

The relative surface energy in the surface area of (2×2) cell with defect to the pure γ-TiAl(111) surface is defined as[34]

$$\gamma_{RS} = (\gamma - \gamma_S) = E^d_{slab} - E^S_{slab} - (N_{Ti} - N^S_{Ti})\mu_{Ti} - (N_{Al} - N^S_{Al})\mu_{Al} - N_O\mu_O, \quad (6)$$

where E^d_{slab} and E^S_{slab} are the total energies of the given configuration with defect and the pure γ-TiAl(111) surface, respectively. At equilibrium, the chemical potential of a given species is equal in all contact phases. This can be used to impose constraints on the possible equilibrium values. In particular, we assume that the surface is in equilibrium with the γ-TiAl bulk, so that $\mu_{Ti}+\mu_{Al}=\mu^{bulk}_{TiAl}$. In order to avoid the formation of metal Ti and Al phases, the chemical potentials must follow $\mu_{Ti} \le \mu^{bulk}_{Ti}$ and $\mu_{Al} \le \mu^{bulk}_{Al}$. Therefore the chemical potential μ_{Al} of Al varies between $\mu^{bulk}_{TiAl} - \mu^{bulk}_{Ti} \le \mu_{Al} \le \mu^{bulk}_{Al}$. The upper limit of the chemical potential of oxygen is determined by the O_2 molecule, so that $\mu_O \le \frac{1}{2}E^t_{O_2}$. Using the *ab initio* computed total energies of the bulk γ-TiAl, Ti, Al, and molecular O_2, we can obtain the chemical-potential ranges of Al and O, $-4.51 \le \mu_{Al} \le -3.69$ eV and $\mu_O \le -4.89$ eV.

III. SELF-SEGREGATION AT THE CLEAN γ-TiAl(111) SURFACE

A. Defect formation energy of the clean γ-TiAl(111) surface

The calculated defect formation energies at the γ-TiAl(111) surface and in γ-TiAl bulk are listed in Table I. From Table I, it can be clearly seen that defect formation energies of Al antisite are lower than that of the other three defects, which suggests that Al antisite defect is more stable than the other kinds of defects. Further inspection of Table I, we can find that the defect formation energy at the second layer and the third layer approaches to that in the bulk, which means that the defect formation energy is determined by the local surroundings. Defect formation energies of Al antisite in the top layer of the surface are negative, which suggests that Al antisite atoms will segregate to the top layer of the surface strongly. The defect formation energy of γ-TiAl(111)-(2×2) surface with one Al antisite at the first surface layer is the lowest (about −0.64 eV) and that at γ-TiAl(111) surface with two Al antisite is the second lowest (about −0.10 eV). Therefore we can conclude that the self-segregation of Al antisite to the first surface layer is very favorable for the clean γ-TiAl(111) surface.

B. Thermodynamic stability of the clean γ-TiAl(111) surface

For further inspection, the calculated relative surface energies of the clean γ-TiAl(111)-(2×2) surface with different surface defects as a function of μ_{Al} are shown in Fig. 2. From Fig. 2, it can be clearly seen that the surface free energy of the γ-TiAl(111)-(2×2) surface with one Al antisite is the lowest over the almost entire range of chemical potential of Al, which indicates that one Al antisite will segregate to the first top layer of the surface easily under this chemical-potential range. This is consistent with the above analysis of defect formation energies. Furthermore, it can be found that for Ti-rich condition the pure γ-TiAl(111) surface is the most stable, while γ-TiAl(111) with two Al antisites is the most stable under Al-rich conditions. So we will mainly investigate the adsorption of oxygen on the pure γ-TiAl(111) surface and segregated-γ-TiAl(111) surface with one or two Al antisites by considering surface segregation effect below. In order to discuss it easily, the segregated-γ-TiAl(111)-(2

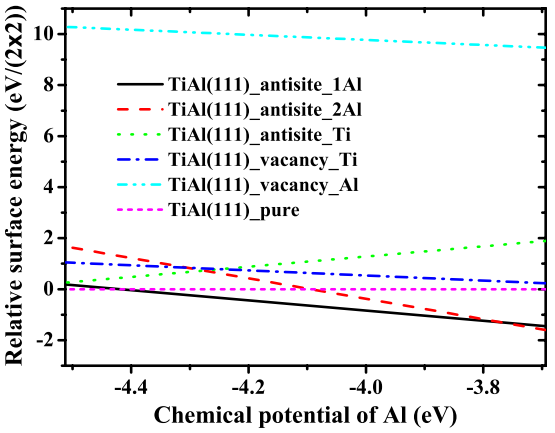

FIG. 2. (Color online) The calculated surface energies of the clean γ-TiAl(111) surface with different surface defects as a function of the chemical potential of Al.

$\times 2$) surface with one and two Al antisites are denoted by γ-TiAl(111)-1Al and γ-TiAl(111)-2Al, respectively. Here, it should be noted that there are three Al atoms and one Ti atom on the first top surface layer for γ-TiAl(111)-1Al surface and a full layer of Al atoms in the first top surface layer for γ-TiAl(111)-2Al surface.

IV. SURFACE SEGREGATION EFFECT ON OXYGEN ADSORBED γ-TiAl(111)

A. Binding energy

The adsorption of oxygen atoms on the pure γ-TiAl(111) surface was investigated for a range of oxygen coverage $0 \leq \Theta \leq 1$. The calculated average binding energies per oxygen atom at different oxygen coverage and adsorption sites are listed in Table II. From Table II, it can be found that for 0.25 ML the most favorable site is fcc-Al site (A_1) followed by hcp-Al (C_1), fcc-Ti (B_1), and hcp-Ti (D_1) sites. The binding energies per oxygen atom at other sites such as top sites and bridge sites are much higher than those of the fcc-Al, fcc-Ti, hcp-Al, and hcp-Ti sites, which are not shown in Table II. Therefore, we just discuss the systems with oxygen atoms taking the four sites as well as their combination. Turning to the higher coverage, the combination of fcc-Al and hcp-Al (A_1+C_1, $A_1+A_1+C_1$, and $A_1+A_1+C_1+C_1$) is the most stable sites for the oxygen coverage $0.50 \leq \Theta \leq 1.00$. It should be mentioned that for the O/γ-TiAl(111) system, the fcc-Al and hcp-Al sites are the sites with more Ti atoms as its nearest neighbors for oxygen adsorption, while the fcc-Ti and hcp-Ti sites are the sites with more Al atoms as its nearest neighbors for oxygen adsorption. As a result, it can be clearly seen that the adsorption site with more Ti atoms as its nearest neighbors on the surface layer is found to be preferred for oxygen adsorption on the pure γ-TiAl(111) surface in the whole discussed coverage. The binding energy per oxygen atom increases when the oxygen coverage is more than 0.75 ML, which reflects the repulsive interaction between the adsorbates with the decrease in O_{A_1}-O_{C_1} distance ($R_{O_{A_1}\text{-}O_{C_1}} = 2.43$ Å). At oxygen coverage of 1.0 ML, the combination of fcc-Al, fcc-Al, fcc-Ti, and fcc-Ti ($A_1+A_1+B_1+B_1$) is almost as stable as the combination of fcc-Al, fcc-Al, hcp-Al, and hcp-Al ($A_1+A_1+C_1+C_1$). These results are in agreement with previous theoretical results of Li *et al.*[14]

As already pointed out in Sec. III, the self-segregation of Al antisite to the first surface layer is very favorable for the clean γ-TiAl(111) surface. Therefore, we study oxygen adsorption on segregated-γ-TiAl(111)-(2×2) surfaces with one or two Al antisites. For γ-TiAl(111)-(2×2) with one Al antisite surface model [see Fig. 1(b)], there are three Al atoms and one Ti atom in the first top surface layer. Therefore, there are two fcc-Al (A_2) sites, two fcc-Ti (B_2, B_2') sites, two hcp-Al (C_2), and two hcp-Ti (D_2, D_2') sites. The different symbols B_2 and B_2' as well as D_2 and D_2' denote the different configurations in the first layer. The calculated binding energy per oxygen atom at different oxygen coverage and adsorption sites for oxygen on the γ-TiAl(111)-1Al surface is listed in Table III. From Table III, it can be found that for 0.25 ML the most favorable site is the fcc-Al (A_2) site followed by hcp-Al (C_2), fcc-Ti (B_2), hcp-Ti (D_2), hcp-Ti (D_2'), and fcc-Ti (B_2') sites. The binding energies per oxygen atom at A_2, B_2, C_2, and D_2 sites with two Al atoms and one Ti atom (2Al-1Ti) surroundings are lower than that of at B_2' and D_2' sites with three Al atoms (3Al) surrounding. Turning to higher coverage, the combination of fcc-Al (A_2) and hcp-Al (C_2) is the most stable site at the oxygen coverage of 0.50 ML. The combination of hcp-Al (C_2), hcp-Al (C_2) and hcp-Ti (D_2) is the most stable site at the coverage of 0.75 ML. However, the combination of fcc-Al (A_2), fcc-Al (A_2),

TABLE II. The calculated binding energies E_b per oxygen atom (eV per atom) on the pure γ-TiAl(111) surface at different adsorption sites for a range of oxygen coverage $0 \leq \Theta \leq 1$.

Site	0.25 ML	Site	0.5 ML	Site	0.75 ML	Site	1.0 ML
A_1	−8.36	A_1+A_1	−8.23	$A_1+A_1+C_1$	−7.93	$A_1+A_1+C_1+C_1$	−7.84
C_1	−8.26	C_1+C_1	−8.18	$A_1+A_1+B_1$	−7.83	$A_1+A_1+B_1+B_1$	−7.83
B_1	−7.46	B_1+B_1	−7.87	$C_1+C_1+D_1$	−7.78	$C_1+C_1+D_1+D_1$	−7.72
D_1	−7.40	D_1+D_1	−7.67	$B_1+B_1+D_1$	−7.63	$B_1+B_1+D_1+D_1$	−7.63
		A_1+C_1	−8.36				
		A_1+B_1	−7.82				
		C_1+D_1	−7.76				
		B_1+D_1	−7.60				

TABLE III. The calculated average binding energy per oxygen atom (eV per atom) on the γ-TiAl(111)-1Al surface for a range of oxygen coverage $0 \leq \Theta \leq 1$ (eV per atom).

Site	0.25 ML	Site	0.50 ML	Site	0.75 ML	Site	1.00 ML
A_2	−7.68	A_2+A_2	−7.60	$A_2+A_2+C_2$	−7.59	$A_2+A_2+C_2+C_2$	−7.74
C_2	−7.66	C_2+C_2	−7.63	$A_2+A_2+B_2$	−7.46	$A_2+A_2+B_2+B_2'$	−7.75
B_2	−7.52	B_2+B_2'	−7.43	$C_2+C_2+D_2$	−7.62	$C_2+C_2+D_2+D_2'$	−7.73
D_2	−7.49	D_2+D_2'	−7.40	$B_2+B_2'+D_2$	−7.27	$B_2+B_2'+D_2+D_2'$	−7.38
B_2'	−6.36	A_2+C_2	−7.76	$A_2+C_2+B_2$	−7.50	$A_2+C_2+B_2+D_2$	−7.51
D_2'	−6.68	A_2+B_2	−7.51				
		A_2+B_2'	−7.50				
		C_2+D_2	−7.56				
		C_2+D_2'	−7.51				
		B_2+D_2	−7.66				
		$B_2'+D_2'$	−6.85				

and hcp-Al (C_2) is not the most stable configuration because of the short distance O_{A_2}-O_{C_2}. For the oxygen coverage of 1.00 ML, the combination of fcc-Al (A_2), fcc-Al (A_2), fcc-Ti (B_2), and fcc-Ti (B_2') is the most stable site, which is slightly more stable than the combination of fcc-Al (A_2), fcc-Al (A_2), hcp-Al (C_2), and hcp-Al (C_2) as well as the combination of hcp-Al (C_2), hcp-Al (C_2), hcp-Ti (D_2), and hcp-Ti (D_2'). This suggests that the adsorption sites of them are all possible for oxygen adsorption at 1.00 ML.

As indicated in Fig. 2, γ-TiAl(111)-(2×2) surface with two Al antisites are stable at Al-rich condition. So we study the oxygen adsorption behavior on γ-TiAl(111)-(2×2) surface with two Al antisites. In this case, all the four atoms in the first top surface layer are Al. The corresponding adsorption sites are denoted by fcc-Al (A_3), fcc-Ti (B_3), hcp-Al (C_3), and hcp-Ti (D_3) shown in Fig. 1(c). The calculated binding energies per oxygen atom at different oxygen coverage and different adsorption sites for oxygen adsorption on γ-TiAl(111)-2Al surface are listed in Table IV. From Table IV, it can be found that for 0.25 ML the most favorable site is the hcp-Al (C_3) site followed by hcp-Ti (D_3), fcc-Al (A_3), and fcc-Ti (B_3). At oxygen coverage of 0.5 ML, the most stable configuration is the combination of two hcp-Al (C_3) sites. Turning to higher coverage, we find that the combination of hcp-Al (C_3) and hcp-Ti (D_3) is the most stable site for the oxygen coverage $0.75 \leq \Theta \leq 1.00$ ML. The binding energy per oxygen atom decreases with the increase in oxygen coverage, which reflects an attractive interaction between oxygen atoms. This behavior is similar to the oxygen adsorption on Al(111) surface.

For further inspection, we also calculate oxygen adsorption on Al(111) surface. The most stable site of oxygen adsorption on Al(111) surface is fcc-hollow site, which is consistent with other theoretical result.[35] In comparison, the binding energies per oxygen atom for O/Ti(0001),[36] O/Al(111), O/γ-TiAl(111), O/γ-TiAl(111)-1Al, and O/γ-TiAl(111)-2Al systems at the most stable site as a function of the oxygen coverage are shown in Fig. 3. From Fig. 3, it can be seen that the binding energy per oxygen atom on Al(111) surface is higher than that on Ti(0001) surface for $0.00 \leq \Theta \leq 1.00$ ML. This may be the reason why the oxygen adsorption site with more Ti atoms as its nearest neighbors is the most stable site for the O/γ-TiAl(111) system at all coverage. The binding energy per oxygen atom of O/Ti(0001) system increases as the oxygen coverage due to a repulsive interaction between adsorbate increases,[36] whereas the binding energy per oxygen atom for O/Al(111) system decreases as the oxygen coverage due to the an attractive interaction between oxygen atoms increases, which is the indicator of formation of alumina island.[35] The trend of the binding-energy curve of oxygen adsorption on γ-TiAl(111)

TABLE IV. The calculated binding energy E_b per oxygen atom (eV per atom) on the γ-TiAl(111)-2Al surface at different adsorption sites for a range of oxygen coverage $0 \leq \Theta \leq 1$.

Site	0.25 ML	Site	0.50 ML	Site	0.75 ML	Site	1.00 ML
A_3	−7.62	A_3+A_3	−7.68	$A_3+A_3+C_3$	−7.85	$A_3+A_3+C_3+C_3$	−7.92
C_3	−7.75	C_3+C_3	−7.86	$A_3+A_3+B_3$	−7.85	$A_3+A_3+B_3+B_3$	−8.11
B_3	−7.34	B_3+B_3	−7.61	$C_3+C_3+D_3$	−8.06	$C_3+C_3+D_3+D_3$	−8.14
D_3	−7.67	D_3+D_3	−7.75	$B_3+B_3+D_3$	−7.56	$B_3+B_3+D_3+D_3$	−7.64
		A_3+C_3	−7.83				
		A_3+B_3	−7.69				
		C_3+D_3	−7.83				
		B_3+D_3	−7.65				

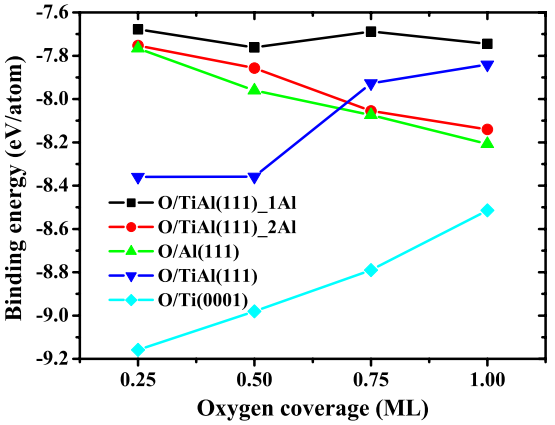

FIG. 3. (Color online) The calculated average binding energies per oxygen atom for the O/Al(111), O/Ti(0001), O/γ-TiAl(111), O/γ-TiAl(111)-1Al, and O/γ-TiAl(111)-2Al systems at the most stable adsorption site as a function of the oxygen coverage.

with Al antisite(s) is closer to that of oxygen adsorption on Al(111) surface as the increase in the surface Al antisites. Especially, the binding-energy curve of O/γ-TiAl(111)-2Al systems is almost the same as that of O/Al(111) system, which may be the formation of pure Al surface layer for γ-TiAl(111)-2Al. Moreover, the binding energy of oxygen on γ-TiAl(111)-2Al decreases with an increase in oxygen coverage, which could benefit the formation alumina island and selective oxidation of aluminum. Further inspection of Fig. 3, we can find that the binding energy per oxygen atom on the γ-TiAl(111)-2Al surface is lower than that of oxygen on the γ-TiAl(111)-1Al surface and also lower than that of oxygen on the pure γ-TiAl(111) surface when the oxygen coverage $\Theta \geq 0.75$ ML. In other words, the O/γ-TiAl(111)-2Al system is the most stable system for $\Theta \geq 0.75$ ML, which suggests that adsorption of oxygen can induce the segregation of another Al antisite at a very high oxygen coverage on the base of the clean γ-TiAl(111)-1Al surface. This will be confirmed by the analysis of thermodynamic stability below.

B. Thermodynamic stability

The calculated relative surface energies for different oxygen coverage and different Al antisite defect γ-TiAl(111) surface systems as a function of μ_O are shown in Figs. 4(a) and 4(b) for Ti-rich and Al-rich conditions, respectively. The calculated phase diagram for oxygen adsorption on the different γ-TiAl(111) surfaces as a function of μ_{Al} and μ_O is shown in Fig. 4(c).

For the Ti-rich condition [Fig. 4(a)], the pure γ-TiAl(111) surface is found to be favored under O-poor conditions, which is consistent with the result of Sec. III B. With an increase in oxygen chemical potential, 0.50 ML oxygen adsorption on pure γ-TiAl(111) surface becomes the most stable. With further increase in oxygen chemical potential, the most stable configuration is the 1.00 ML oxygen adsorption on the pure γ-TiAl(111) surface. The adsorption of oxygen on the surfaces with Al antisites is not favorable under the Ti-rich condition.

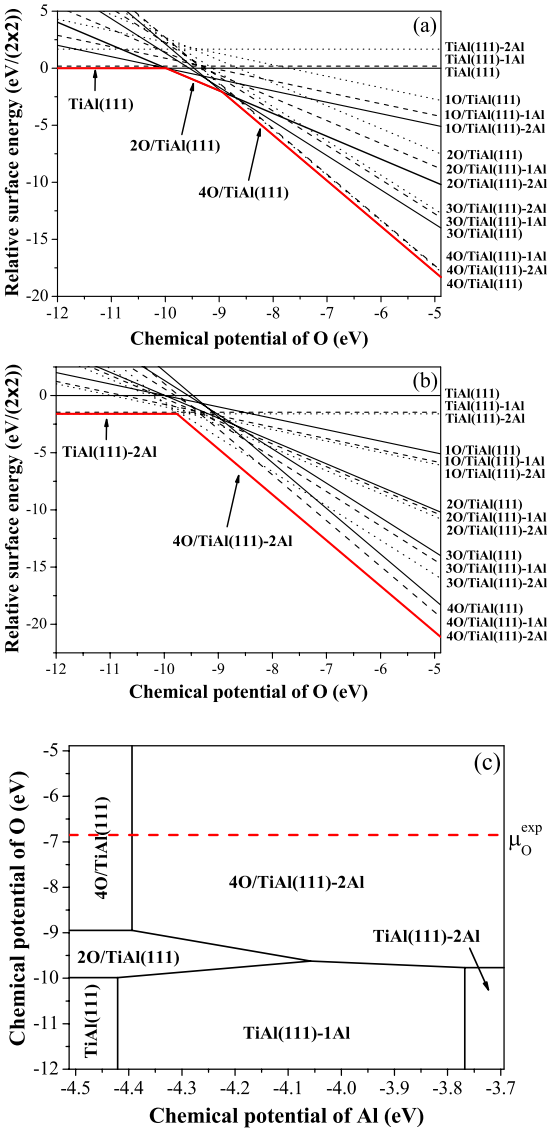

FIG. 4. (Color online) The relative surface energies of oxygen covered surfaces under (a) Ti-rich and (b) Al-rich conditions. (c) illustrates the calculated phase diagram for oxygen adsorption on the different γ-TiAl(111) surfaces as a function of μ_{Al} and μ_O. TiAl(111), TiAl(111)-1Al, and TiAl(111)-2Al represent the clean, with one, and with two Al antisite defects TiAl(111) surface in a 2×2 unit cell, respectively. 1O, 2O, 3O, and 4O represent one, two, three, and four oxygen atom adsorptions on the corresponding TiAl surface in a 2×2 unit cell, which correspond to 0.25, 0.50, 0.75, and 1.0 ML oxygen coverage, respectively. The dashed line in (c) represents the chemical potential of oxygen at the experimental conditions (Refs. 11 and 12).

For Al-rich condition [Fig. 4(b)], the most stable surface configuration under O-poor condition corresponds to the γ-TiAl(111)-2Al surface, which is also consistent with the result of Sec. III B. With the increase in oxygen chemical potential, the oxygen adsorption on the γ-TiAl(111)-2Al surface with the oxygen coverage of 1.00 ML becomes the most stable configuration.

For further inspection, the calculated phase diagram for oxygen adsorption on the different γ-TiAl(111) surfaces as a

function of μ_{Al} and μ_O is shown in Fig. 4(c). This phase diagram is drawn in the chemical-potential space. It shows the most stable configuration for different values of μ_{Al} and μ_O. From Fig. 4(c), under low oxygen chemical-potential condition, most of the part of Al chemical-potential space is occupied by the γ-TiAl(111)-1Al surface, while the very small part of Al chemical-potential space is occupied by the pure γ-TiAl(111) surface under low Al chemical-potential condition and γ-TiAl(111)-2Al under high Al chemical-potential condition, respectively. It means that the clean surface without oxygen adsorption is the most possible configuration under O-poor condition. Under the condition of high O chemical potential and high Al chemical potential, the γ-TiAl(111)-2Al surface adsorbed with 1.0 ML oxygen is the most stable configuration and has the largest area in the phase diagram. The O-induced Al segregation on the γ-TiAl(111) surface can take place when the chemical potential of oxygen is high enough ($\mu_O \geq -9.77$ eV), even under the Al-poor condition (at $-4.39 \leq \mu_{Al} \leq -4.06$ eV). O-induced Al segregation behavior also exists in the binding-energy results in Sec. IV A. From the point of nonstoichiometries view, even a slight Al-rich condition in the nominally ordered γ-TiAl bulk can benefit the segregation of Al antisites for the clean surface and oxygen adsorbed system. In other words, one Al antisite surface segregation is due to self-segregation of clean surface; another Al antisite surface segregation can be induced by the oxygen adsorption. The segregation of two Al antisites in the first top surface layer at the γ-TiAl(111)-(2×2) surface could achieve the pure full Al surface layer. Therefore this dramatic effect of complete surface segregation of two Al antisites could promote the selective oxidation of aluminum.

In order to compare our theoretical results with the experiments in detail,[11,12] we calculate the chemical potential of oxygen as a function of temperature T and oxygen partial pressure P with the following formula:[37]

$$\mu_O(T,P) = \frac{1}{2}E^t_{O_2} + \mu_O(T,P^0) + \frac{1}{2}k_B T \ln\left(\frac{P}{P^0}\right), \qquad (7)$$

where $E^t_{O_2}$ is the total energy of an isolated oxygen molecule. $\mu_O(T,P^0)$ is the chemical potential of oxygen at temperature T and pressure P^0, which could be obtained from experimental data as given in standard thermodynamic tables.[38] Therefore the chemical potential of oxygen under the experimental conditions ($T=650$ °C$=923$ K and $P=1.0\times10^{-7}$ mbar)[11,12] can be obtained, $\mu_O^{expt}=-6.81$ eV. This value is presented by a dashed line in Fig. 4(c), which corresponds to the high O chemical potential. In addition, the chemical potential of Al in γ-TiAl with stoichiometric composition in experiment is about in middle of the whole range of chemical potential of Al in Fig. 4(c). As a result, from Fig. 4(c), it can be clearly seen that, under experimental oxygen gas environment and stoichiometric composition of γ-TiAl conditions, the γ-TiAl(111)-2Al surface adsorbed with 1.0 ML oxygen is the most stable configuration, which could perform selective oxidation of aluminum. This may help to explain the growth of pure alumina layer originating from the selective oxidation of aluminum on the γ-TiAl(111) surface at the first stage in the experiments.[11,12]

C. Atomic structure

In order to study the surface segregation effect on atomic structure of oxygen adsorbed systems, the relaxed atomic structure for O/γ-TiAl(111), O/γ-TiAl(111)-1Al, and O/γ-TiAl(111)-2Al systems at the most stable site with the different oxygen coverage are listed in Table V. We calculate the minimal O-Ti separation $R_{O\text{-}Ti}$ and the minimal O-Al separation $R_{O\text{-}Al}$ both in three-dimensional (3D) space and along the direction normal to the surfaces $Z_{O\text{-}Ti}$ and $Z_{O\text{-}Al}$. We also calculate the surface ripple between Al and Ti in the first layer near oxygen atom as a definition of $\Delta Z = Z_{Ti} - Z_{Al} = Z_{O\text{-}Al} - Z_{O\text{-}Ti}$. Negative and positive values of ΔZ correspond to Al and Ti atoms' upward surfaces, respectively.

Comparing atomic structures for different systems in Table V, we can find that the O-Al distances ($R_{O\text{-}Al}$ and $Z_{O\text{-}Al}$) for oxygen adsorbed γ-TiAl(111) surface with Al antisite defect become shorter than those for the oxygen adsorbed pure γ-TiAl(111) surface. Meanwhile, the O-Ti distances ($R_{O\text{-}Ti}$ and $Z_{O\text{-}Ti}$) for oxygen adsorbed γ-TiAl(111) surface with Al antisite defect become longer than those for oxygen adsorbed pure γ-TiAl(111) surface. This indicates that the interaction between O atom and Al (Ti) atom is stronger (weaker) in the surfaces with Al antisite than that in the pure surface. This will be supported by the analysis of projected density of states in Sec. IV D. For the clean systems, the first top surface layer ripple ΔZ between Al and Ti for both clean γ-TiAl(111) and γ-TiAl(111)-1Al surfaces is negative, which indicates that the positions of Al atoms are upper than those of Ti atoms. Furthermore, the first surface layer ripple ΔZ of oxygen covered pure γ-TiAl(111) surface increases from a negative value to a positive value as the oxygen coverage increases, which indicates oxygen could induce the top layer from Al upward to Ti upward with the increase in oxygen coverage. For oxygen covered γ-TiAl(111)-1Al surface, the surface ripple ΔZ becomes smaller compared with the corresponding values of oxygen covered pure γ-TiAl(111) surface. It is the Al antisite that makes oxygen atom interaction with surface Al atoms becomes stronger relative to the O/TiAl(111) system. For the O/TiAl(111)-2Al system, it can be found that the O-Al distances $R_{O\text{-}Al}$ and $Z_{O\text{-}Al}$ become shorter with the increase in the oxygen coverage. It indicates that the interaction between O and Al becomes stronger with the increase in oxygen coverage. This may be the reason why the binding energy of oxygen adsorbed on γ-TiAl(111)-2Al decreases with the increase in oxygen coverage.

D. Density of states

In order to understand the surface segregation effect on bonding behavior of oxygen atom with the substrate, projected densities of states (PDOSs) are calculated. In this part, we mainly discuss the cases of the oxygen adsorbed systems with the coverage $\Theta=0.25$ and 1.00 ML. The PDOSs of O/γ-TiAl(111), O/γ-TiAl(111)-1Al, and O/γ-TiAl(111)-2Al systems with 0.25 ML are shown in

TABLE V. The calculated structure parameters (in angstrom) for oxygen adsorption on pure γ-TiAl(111), γ-TiAl(111)-1Al, and γ-TiAl(111)-2Al surfaces at the most stable site with different coverage. Here, we also define the ripple between Al and Ti in the first surface layer ($\Delta Z_{\text{Ti-Al}}$): $\Delta Z_{\text{Ti-Al}}=Z_{\text{Ti}}-Z_{\text{Al}}=Z_{\text{O-Al}}-Z_{\text{O-Ti}}$.

Θ (ML)	Surface	Site	$R_{\text{O-Al}}$	$R_{\text{O-Ti}}$	$Z_{\text{O-Al}}$	$Z_{\text{O-Ti}}$	$\Delta Z_{\text{Ti-Al}}$
0.00	γ-TiAl(111)						−0.173
	γ-TiAl(111)-1Al						−0.266
	γ-TiAl(111)-2Al						
0.25	γ-TiAl(111)	fcc-Al	1.875	1.955	0.941	1.058	−0.117
	γ-TiAl(111)-1Al	fcc-Al	1.855	1.976	0.779	1.081	−0.302
	γ-TiAl(111)-2Al	hcp-Al	1.854		0.739		
0.50	γ-TiAl(111)	fcc-Al	1.847	1.935	1.089	1.014	0.075
		hcp-Al	1.804	1.952	0.927	0.851	0.076
	γ-TiAl(111)-1Al	fcc-Al	1.828	1.981	0.967	1.029	−0.062
		hcp-Al	1.810	1.944	0.772	0.834	−0.062
	γ-TiAl(111)-2Al	hcp-Al	1.834		0.752		
		hcp-Al	1.834		0.752		
0.75	γ-TiAl(111)	fcc-Al	1.864	1.901	1.232	0.883	0.349
		hcp-Al	1.756	1.973	1.011	0.661	0.350
	γ-TiAl(111)-1Al	hcp-Al	1.770	1.997	0.580	1.066	−0.486
		hcp-Ti	1.778	3.501	0.733	1.219	−0.486
	γ-TiAl(111)-2Al	hcp-Al	1.811		0.720		
		hcp-Ti	1.817		0.795		
1.00	γ-TiAl(111)	fcc-Al	1.823	1.932	1.440	0.789	0.651
		hcp-Al	1.742	1.942	0.946	0.295	0.651
	γ-TiAl(111)-1Al	fcc-Al	1.822	1.851	0.924	0.819	0.105
		fcc-Ti	1.790	1.879	0.578	0.561	−0.017
	γ-TiAl(111)-2Al	hcp-Al	1.789		0.633		
		hcp-Ti	1.794		0.772		

Figs. 5(a)–5(c), respectively. The PDOSs of O/γ-TiAl(111) and O/γ-TiAl(111)-2Al systems with 1.00 ML are shown in Figs. 5(d) and 5(e), respectively.

For the O/γ-TiAl(111) [Fig. 5(a)] system, O_{2p} states interact with Al_{3p} and $Ti_{4p,3d}$ at about −4.7 eV; O_{2s} states interact with $Al_{3s,3p}$ and $Ti_{4s,4p,3d}$ at about −19 eV. However, when oxygen atom adsorbed on γ-TiAl(111)-(2×2) with one Al antisite surface [Fig. 5(b)], the O_{2p} states split into two peaks at about −4.7 and −6.3 eV. Besides the interactions between O_{2p} and Al_{3p} states at −4.7 eV as existed in the O/γ-TiAl(111) system, there are interactions between O_{2p} and Al_{3s} at −6.3 eV. As a result, the interactions between O and Al atoms in O/γ-TiAl(111)-1Al are stronger than those in O/γ-TiAl(111) system. For the O/γ-TiAl(111)-2Al system with oxygen coverage of 0.25 ML, the energy levels of O_{2s} and Al_{3s} states are shifted downward further.

Turning to high oxygen coverage of 1.0 ML, the similar feature with that of oxygen coverage of 0.25 ML can be found. For the O/γ-TiAl(111) system [Fig. 5(d)], O_{2p} states interact with Al_{3p} and $Ti_{4p,3d}$ in the energy range from −1.5 to −7.0 eV; O_{2s} states interact with $Al_{3s,3p}$ and $Ti_{4s,4p,3d}$ at about −18 eV. For the O/γ-TiAl(111)-2Al system [Fig. 5(e)], two peaks appear at about −5.0 and −7.8 eV in O_{2p} states. The states of O_{2p} strongly interact with Al_{3s} and Al_{3p} states at these energy levels. The O_{2s} states at lower energy level of −20.0 eV interact with states of $Al_{3s,3p}$. The energy levels for the O/γ-TiAl(111)-2Al system [see Fig. 5(e)] are shifted downward compared with those of the O/γ-TiAl(111) system [see Fig. 5(d)], which also indicates that the interactions between O and Al atoms are stronger than those in the O/γ-TiAl(111) system. The PDOS results indicate that the bonding between O and Al becomes stronger with the increase in the oxygen coverage, which is consistent with the above analysis of atomic structure and binding energies results.

V. CONCLUSION

In this work, the surface self-segregation effect on the oxygen adsorption at the γ-TiAl(111) surface as well as sur-

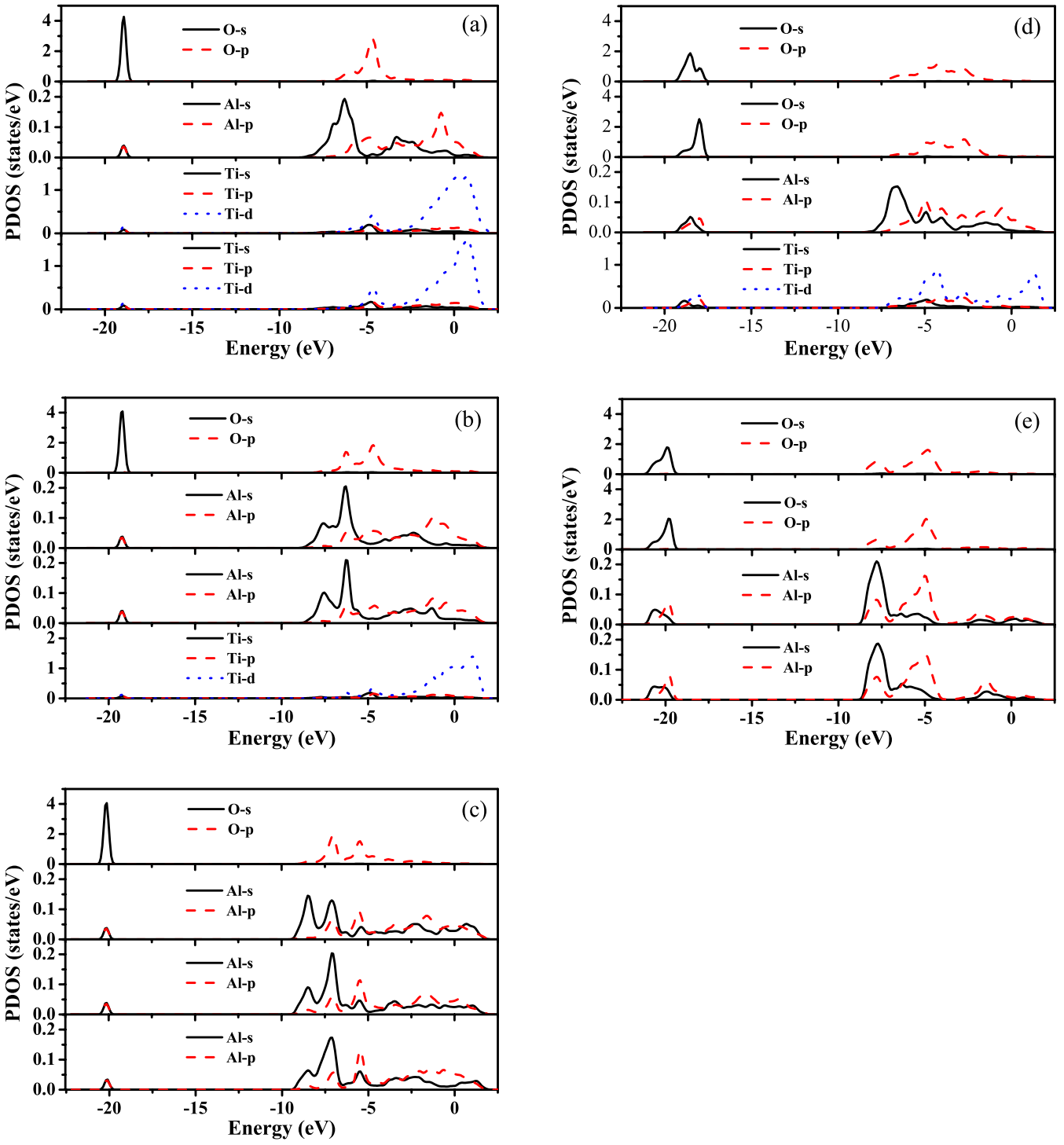

FIG. 5. (Color online) The PDOS of oxygen and surface atoms in the different systems: (a) O/ γ-TiAl(111) with 0.25 ML, (b) O/ γ-TiAl(111)-1Al with 0.25 ML, (c) O/ γ-TiAl(111)-2Al with 0.25 ML, (d) O/ γ-TiAl(111) with 1.00 ML, and (e) O/TiAl(111)-2Al with 1.00 ML at the most stable adsorption sites. The *s*, *p*, and *d* states are indicated by solid, dashed, and dotted lines, respectively. The zero energy corresponds to the Fermi level.

face phase diagram was studied by plane-wave-pseudopotential VASP codes based on the density-functional theory. For the pure γ-TiAl(111) surface, the most stable oxygen adsorption sites are the sites with more Ti atoms as the neighbors of oxygen atoms in agreement with previous calculations. The defect formation energy and relative surface energy results show that the Al antisite defect can appear at the γ-TiAl(111) surface. Especially, under Al-rich condition, γ-TiAl(111)-(2×2) with two Al antisites defect is the most stable configuration. In this case, the first surface layer of γ-TiAl(111)-(2×2) surface is completely composed of Al atoms. The adsorption behaviors of oxygen on the

γ-TiAl(111)-(2×2) surface with one Al antisite and two Al antisites are compared with those of oxygen adsorption on Ti(0001) and Al(111) surfaces. The oxygen adsorption behavior on the γ-TiAl(111)-(2×2) surface with two Al antisites is very similar to that on Al(111) surface: the binding energy per oxygen atom decreases with the increase in the oxygen coverage, which may benefit the formation of alumina island and the selective oxidation of aluminum. Moreover, the stability of O/γ-TiAl(111)-(2×2) surfaces with different oxygen coverage and different Al antisite defects is studied by relative surface energy. From the thermodynamics point of view, under Ti-rich condition, the most stable configuration is the clean γ-TiAl(111) surface at low oxygen chemical potential, then at 0.5 ML, and finally at 1.0 ML oxygen adsorption on the γ-TiAl(111) surface with the increase in oxygen chemical potential. This means that under Ti-rich condition the occurrence of Al antisite defect on this surface is impossible. However, under Al-rich condition, the most stable configuration is γ-TiAl(111)-(2×2) with two Al antisites at low oxygen chemical potential then at 1.0 ML oxygen adsorption on γ-TiAl(111)-(2×2) with two Al antisites. The atomic geometry and density-of-states analysis indicate that the interaction between O and Al atoms becomes stronger with the increase in the Al content at the first layer of the γ-TiAl(111) surface. As a result, this dramatic effect of Al surface segregation could promote the selective oxidation of aluminum, which is consistent with the growth of pure alumina layer originating from the selective oxidation of aluminum on the γ-TiAl(111) surface at the first stage in the experiments.

ACKNOWLEDGMENTS

This work was supported by the Foundation for National Excellent Doctoral Dissertations of China under Grant No. 200334 and National Natural Science Foundation of China under Grant No. 50871071.

*Author to whom correspondence should be addressed; shangjx@buaa.edu.cn

[1] F. H. Froes, C. Suryanarayana, and D. Eliezer, J. Mater. Sci. **27**, 5113 (1992).
[2] E. A. Loria, Intermetallics **8**, 1339 (2000).
[3] H. Clemens and H. Kestler, Adv. Eng. Mater. **2**, 551 (2000).
[4] A. Rahmel, W. J. Quadakkers, and M. Schütze, Mater. Corros. **46**, 217 (1995).
[5] S. Becker, A. Rahmel, W. J. Quadakkers, and M. Schütze, Oxid. Met. **38**, 425 (1992).
[6] C. Lang and M. Schütze, Oxid. Met. **46**, 255 (1996).
[7] C. Lang and M. Schütze, Mater. Corros. **48**, 13 (1997).
[8] M. Schmitz-Niederau and M. Schütze, Oxid. Met. **52**, 225 (1999).
[9] K. Maki, M. Shioda, M. Sayashi, T. Shimizu, and S. Isobe, Mater. Sci. Eng., A **153**, 591 (1992).
[10] Y. Shida and H. Anada, Mater. Trans., JIM **35**, 623 (1994).
[11] V. Maurice, G. Despert, S. Zanna, M.-P. Bacos, and P. Marcus, Nature Mater. **3**, 687 (2004).
[12] V. Maurice, G. Despert, S. Zanna, M.-P. Bacos, and P. Marcus, Surf. Sci. **596**, 61 (2005).
[13] V. Maurice, G. Despert, S. Zanna, P. Josso, M.-P. Bacos, and P. Marcus, Acta Mater. **55**, 3315 (2007).
[14] H. Li, L. M. Liu, S. Q. Wang, and H. Q. Ye, Acta Metall. Sin. **42**, 897 (2006).
[15] V. Blum, L. Hammer, C. Schmidt, W. Meier, O. Wieckhorst, S. Müller, and K. Heinz, Phys. Rev. Lett. **89**, 266102 (2002).
[16] L. V. Pourovskii, A. V. Ruban, B. Johansson, and I. A. Abrikosov, Phys. Rev. Lett. **90**, 026105 (2003).
[17] A. Y. Lozovoi, A. Alavi, and M. W. Finnis, Phys. Rev. Lett. **85**, 610 (2000).
[18] P. Hohenberg and W. Kohn, Phys. Rev. **136**, B864 (1964).
[19] W. Kohn and L. J. Sham, Phys. Rev. **140**, A1133 (1965).
[20] G. Kresse and J. Hafner, Phys. Rev. B **48**, 13115 (1993).
[21] G. Kresse and J. Furthmüller, Phys. Rev. B **54**, 11169 (1996).
[22] G. Kresse and J. Furthmüller, Comput. Mater. Sci. **6**, 15 (1996).
[23] J. P. Perdew, J. A. Chevary, S. H. Vosko, K. A. Jackson, M. R. Pederson, D. J. Singh, and C. Fiolhais, Phys. Rev. B **46**, 6671 (1992).
[24] P. E. Blöchl, Phys. Rev. B **50**, 17953 (1994).
[25] G. Kresse and D. Joubert, Phys. Rev. B **59**, 1758 (1999).
[26] E. A. Brandes, *Smithell Metals Reference Book*, 6th ed. (Butterworth, London, 1983).
[27] R. Benedek, A. van de Walle, S. S. A. Gerstl, M. Asta, D. N. Seidman, and C. Woodward, Phys. Rev. B **71**, 094201 (2005).
[28] J. Neugebauer and M. Scheffler, Phys. Rev. B **46**, 16067 (1992).
[29] L. Bengtsson, Phys. Rev. B **59**, 12301 (1999).
[30] G. X. Qian, R. M. Martin, and D. J. Chadi, Phys. Rev. B **38**, 7649 (1988).
[31] J. E. Northrup, Phys. Rev. Lett. **62**, 2487 (1989).
[32] H. Z. Zhang and S. Q. Wang, Acta Mater. **55**, 4645 (2007).
[33] J. R. Kitchin, K. Reuter, and M. Scheffler, Phys. Rev. B **77**, 075437 (2008).
[34] F. H. Wang, P. Krüger, and J. Pollmann, Phys. Rev. B **64**, 035305 (2001).
[35] A. Kiejna and B. I. Lundqvist, Phys. Rev. B **63**, 085405 (2001).
[36] S. Y. Liu, F. H. Wang, Y. S. Zhou, and J. X. Shang, J. Phys.: Condens. Matter **19**, 226004 (2007).
[37] K. Reuter and M. Scheffler, Phys. Rev. B **65**, 035406 (2001).
[38] D. R. Stull and H. Prophet, *JANAF Thermochemical Tables*, 2nd ed. (U.S. National Bureau of Standards, Washington, DC, 1971).